Ozone mediated depolymerization and solvolysis of technical lignins under ambient conditions in ethanol

Bernardes Figueiredo, M. B.; Heeres, H. J.; Deuss, P. J.

Published in:
Sustainable Energy & Fuels

DOI:
10.1039/C9SE00740G

Publication date:
2020

Sustainable Energy & Fuels

PAPER

View Article Online
View Journal | View Issue

Cite this: *Sustainable Energy Fuels*, 2020, **4**, 265

Ozone mediated depolymerization and solvolysis of technical lignins under ambient conditions in ethanol†

M. B. Figueirêdo, H. J. Heeres and P. J. Deuss *

Technical lignins are highly available and inexpensive feedstocks derived from current large scale biomass utilizing industries. Their valorization represents a bottleneck in the development of biorefineries, as the inherently complex lignin structure often suffers severe condensation during isolation, leading to their current application as low value fuel. Processes able to depolymerize technical lignins into value-added (intermediate) molecules are of great interest for the development of integrated, viable routes aiming at the full valorization of lignocellulosic biomass. Here, we report an effective ozone mediated depolymerization of four technical lignins (Indulin-AT Kraft, ball-milled Indulin-AT Kraft, Alcell organosolv and Fabiola organosolv) in ethanol under ambient conditions without the need for catalysts. 52–87 wt% of these nearly ethanol insoluble lignins was broken down into soluble fragments upon ozone exposure. The average molecular weight of the soluble fragments was shown to have decreased by 40–75% compared to the parent materials. A range of (di)carboxylic acids and (di)ethyl esters was identified, accounting for up to 40 wt% of the ozonated lignin oils. These products are the result of phenol ring-opening reactions as well as oxidative cleavage of unsaturated linking motifs followed by partial esterification. Reactivity varied substantially among the lignin feedstocks. For instance, lower particle sizes and higher degradation of the native lignin structure were shown to be beneficial for the effective action of the ozone. Our results show that a straightforward ozonation process under ambient conditions can depolymerize recalcitrant lignins into oxygenated fragments and low molecular weight products soluble in ethanol. These can potentially be used for the synthesis of high-value drop-in chemicals.

Received 2nd September 2019
Accepted 1st November 2019

DOI: 10.1039/c9se00740g

rsc.li/sustainable-energy

Introduction

Lignin is one of the three main fractions of lignocellulosic biomass, corresponding to up to 40 wt% and consists in its native form of a highly crosslinked and methoxylated phenylpropanoid network (Fig. 1A).[1] Compared to the carbohydrate fraction, lignin is largely unutilized and often burned for low value energy generation.[2] The complex structure of this biopolymer suffers severe degradation during isolation in typical industrial processes, *e.g.* Kraft for pulp and paper production.[3,4] This makes further valorization of these so-called technical lignins (produced at large scales, *e.g.* 50 million tons per year of Kraft lignin[5]) *via* depolymerization challenging.[6] Technical lignins are highly condensed and chemically heterogeneous, with substantially lower amounts of the labile C–O linkages present in abundance in native lignin[7,8] (Fig. 1B). Within the biorefinery concept, which aims to achieve full

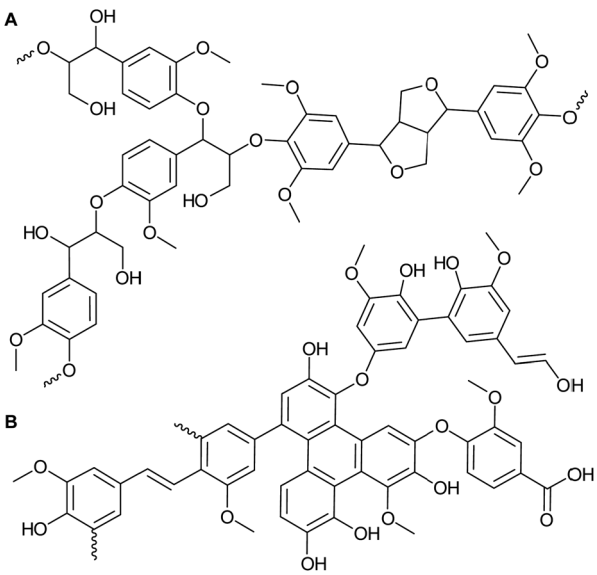

Fig. 1 Structural models of native lignin (A) and technical lignin (B).

Department of Chemical Engineering (ENTEG), University of Groningen, Nijenborgh 4, Groningen, 9747 AG, the Netherlands. E-mail: p.j.deuss@rug.nl

† Electronic supplementary information (ESI) available. See DOI: 10.1039/c9se00740g

valorization of biomass by converting all of its fractions into value-added chemicals, materials and fuels, lignin stands as a promising source of renewable carbon.[1,9] Therefore, the development of processes able to deconstruct the recalcitrant structure of technical lignins to yield value-added (intermediate) chemicals is of great interest.

Several strategies for the depolymerization of technical lignins have been suggested. For instance, catalytic hydrotreatment has been widely studied to hydrodeoxygenate and hydrocrack lignin to yield fuels and chemicals. A range of heterogeneous catalysts have been reported with and without the use of solvents, *e.g.* CoMo and NiMo supported catalysts typically used in petro-based refineries,[10–12] noble metal supported catalysts,[13–18] inexpensive iron ores[19,20] and catalysts based on transition metals such as Ni.[21–27] Despite the high monomer yields of up to 35 wt% observed (largely comprised of aromatics and alkylphenolics), costs related to hydrogen and catalysts are still impeditive, harsh reaction conditions are typically needed (*i.e.* temperatures > 350 °C, high pressures) and significant carbon losses to solids and the gas phase occur.

Oxidative depolymerization strategies have also been reported for lignin valorization, using oxygen, air and hydrogen peroxide as typical oxidants. Various catalytic systems have been investigated, in which homogeneous catalysts are often employed, *e.g.* TEMPO[28,29] and polyoxometalates.[30–32] Heterogeneous catalysts (*e.g.* chalcopyrite,[33] metal-supported,[34] metal oxides,[35] metal composites,[36] hydrotalcites[37]) and new approaches using biomimetic catalysts,[38,39] anchored TEMPO[40] and ionic liquids[41–43] have been explored as well. The applied conditions are usually milder than those employed in reductive strategies. Products derived from lignin oxidation include aromatic acids and aldehydes, phenolic building blocks and dicarboxylic acids (DCAs) with several potential applications as specialty and platform chemicals, fuels and additives. Overall, the use of catalysts adds extra complexity to lignin processing due to separation and reusability difficulties, fast deactivation, poisoning, high costs and irreversible morphologic changes in the case of heterogeneous catalysts.[44] Non-catalytic routes for the upgrading of technical lignins include pyrolysis[45–47] and solvolysis,[48–52] which despite the promising results, also need high temperatures to efficiently break down the structure and minimize repolymerization pathways. In addition, low monomer yields and high carbon losses to the gas, solid and aqueous phases are common.

Ozonation is a less explored process for lignin valorization, despite the high reactivity of ozone towards lignin-like structures at mild conditions without the need of catalysts.[53,54] Ozone can be easily generated *in situ*, either from oxygen or dry air, and technology is well-established and available at all scales. Furthermore, ozone has a short half-life, thus any residual ozone in the system quickly decomposes to O_2, which facilitates safe operation. This provides an overall clean procedure that does not need further separation steps to remove reagents.[55] Previous studies showed that ozonated biomass solutions contain a range of aromatic aldehydes, quinones and carboxylic acids derived from the lignin fraction.[33,56,57] An investigation of alkali lignin ozonation reported that the thus produced esters are suitable for applications as fuel additives.[55] In another study, ozonated lignin was shown to be suitable for the production of vitrimer materials with potential use as recoverable adhesives.[58] Recent publications from our group[59,60] showed the potential of pyrolytic lignin (PL) ozonation for the production of biobased DCAs and methyl esters at mild conditions (*i.e.* 0 °C and atmospheric pressure), having methanol as solvent. In addition, model compound studies also showed the high reactivity of ozone towards phenolic motifs and unsaturated C–C bonds. These results inspired us to move from low molecular weight PL's to more complex and degraded lignin feeds, which are known to contain high amounts of the said functionalities,[61] using even milder conditions (Fig. 2).

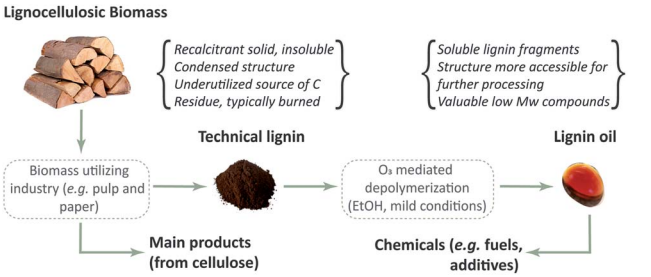

Fig. 2 Scheme of the ozone mediated depolymerization process here reported.

Thus, here we report the depolymerization and subsequent dissolution of four initially ethanol insoluble technical lignins by a simple ozone treatment. All experiments were performed under ambient conditions at relatively short reaction times of under two hours, using absolute ethanol as the solvent. The use of ethanol is advantageous over methanol due to its very low toxicity and biobased character. Two types of lignin feeds were chosen based on their high industrial availability and challenging structure,[5] *i.e.* Kraft lignin (Indulin-AT, abbreviated here as KL) and Alcell organosolv lignin.[62] Our studies show that ozone is remarkably effective for the depolymerization and solubilization of these lignins. A ball-milled KL was added to the scope to evaluate the particle size influence on the process. Furthermore, Fabiola lignin, which is an organosolv lignin obtained under milder conditions than the Alcell,[63] was also evaluated to get insights on the influence of lignin condensation on the ozonation extent.

Materials and methods

Chemicals

Indulin-AT (Kraft lignin, KL) was supplied by MeadWestvaco Specialty Chemicals, USA. Indulin-AT is a purified form of pine-derived KL and does not contain hemicellulose. The ball-milled KL was obtained by ball milling KL for 30 minutes at 1200 RPM (Retsch 400). The Alcell (ethanosolv from a mixture of hardwoods) and Fabiola (acetosolv from beech wood) organosolv

lignins were supplied by ECN-TNO. The extraction procedure and associated conditions of the latter are described elsewhere.[63] All lignins were obtained in powder form and their particle sizes were determined by dynamic light scattering (DLS). Tetrahydrofuran (THF), toluene, ethanol, deuterated dimethyl sulfoxide (DMSO-d_6), deuterated chloroform ($CDCl_3$), pyridine, cyclohexanol, chromium(III) acetylacetonate and 2-chloro-4,4,5,5-tetramethyl-1,3,2-dioxaphopholane were purchased from Sigma-Aldrich. All chemicals in this study were used as received.

Ozonation experiments

The ozonation experiments were performed under ambient conditions. A 100 mL round bottom flask containing a magnetic stirrer was used. 2 g of lignin and 45 g of ethanol were added in each experiment. For the longer experiments of 120 minutes, 2 g of lignin and 60 g of ethanol were used. Ozone (diluted in oxygen) was bubbled in the mixture through a pipette. A flow of 4 L min^{-1} of oxygen was fed into the ozone generator (model LAB2B from Ozonia), producing 9.5 g of O_3 per h. Stirring was set to 1500 RPM. The reaction time varied from 20 to 120 min, while all other process parameters were kept constant. After each reaction, the oxidized mixture was flushed with air for around 2 minutes to remove residual ozone and filtered for the recovery of solids. Ethanol was removed by vacuum evaporation (2 h, 250 mbar and 40 °C) to yield the final lignin oil, which was weighted and analyzed in detail.

Since the evaluated lignins have very low solubility in ethanol and the solvent participates in the ozonation to some extent (*vide infra*), the amounts of dissolved lignin and mass incorporation were calculated based on the solids recovered after each reaction (here called insoluble lignin). Hence, these solids were considered unreacted lignin and provided an indication of how much of the initial lignin was extracted to the solvent during ozonation (*i.e.* dissolved lignin). By knowing the amount of dissolved lignin, the mass incorporation could be quantified as well (eqn (1) and (2)). For a better comparison between the experiments, an incorporation ratio (IR) factor was defined (eqn (3)). The reader is referred to the ESI† for an example of calculations using the data obtained from a typical ozonation experiment.

$$\text{Insoluble lignin} = \text{initial lignin} - \text{dissolved lignin} \quad (1)$$

$$\text{Lignin oil} = \text{mass incorporation} + \text{dissolved lignin} \quad (2)$$

$$\text{Incorporation ratio (IR)} = \frac{\text{lignin oil}}{\text{dissolved lignin}} \quad (3)$$

CAUTION: Ozone is a highly reactive and toxic gas. Chronic exposure and exposure to high concentrations of ozone may cause respiratory difficulties and eye irritation. The apparatus described in this report should only be operated with proper ventilation in a fume hood. Generation of ozone requires a high-voltage discharge, therefore care is advised to isolate the high-voltage components of the apparatus from any nearby solvents.

Feed and lignin oil analyses

Prior to the ozonation experiments, the four lignin feeds were characterized by GPC (weight average molecular weight, M_w), HSQC NMR (linking motifs as well as the aromatic unit composition syringyl/guaiacyl/*p*-hydroxybenzene S/G/H ratio), ^{13}C-NMR (overall chemical makeup of carbons), ^{31}P-NMR (hydroxyl types and content), elemental analysis (C, H, N, S) and DLS (particle size). The chemical composition of the ozonated lignin oils was also assessed by a series of techniques; GPC (M_w and molecular weight distribution), TGA (charring tendency and volatility), GC-MS (identification of thermally stable monomers), HPLC (carboxylic acids identification and quantification), HSQC NMR and ^{13}C-NMR (structural features), Karl Fischer analysis (water content) and elemental composition (C, H, N, S elemental analyzer). pH measurements of the ethanol and KL mixtures before and after ozonation (diluted 50 wt% in water) were performed using a 848 Titrino plus apparatus from Metrohm.

GPC analyses of the feed and products were performed using an Agilent HPLC 1100 system equipped with a refractive index detector. Three columns in series of MIXED type E (length 300 mm, i.d. 7.5 mm) were used. Polystyrene standards were used for calibration. 0.05 g of the sample was dissolved in 4 mL of THF together with 2 drops of toluene as the external reference and filtered (filter pore size 0.45 μm) before injection.

Thermogravimetric analyses (TGA) were performed using a TGA 7 from PerkinElmer. The samples were heated under a nitrogen atmosphere (nitrogen flow of 50 mL min^{-1}), with heating rate of 10 °C min^{-1} and temperature ramp of 30–900 °C.

Gas chromatography/mass spectrometry (GC-MS) analyses were performed on a Hewlett-Packard 5890 gas chromatograph equipped with a RTX-1701 capillary column (30 m × 0.25 mm i.d. and 0.25 μm film thickness) and a Quadrupole Hewlett-Packard 6890 MSD selective detector attached. Helium was used as carrier gas (flow rate of 2 mL min^{-1}). The injector temperature was set to 280 °C. The oven temperature was kept at 40 °C for 5 minutes, then increased to 250 °C at a rate of 3 °C min^{-1} and held at 250 °C for 5 minutes. All samples were diluted 10 times with THF.

The HPLC analytical device used for carboxylic acids identification and quantification consisted of an Agilent 1200 pump, a Bio-Rad organic acids column Aminex HPX-87H, a Waters 410 differential refractive index detector and a UV detector. The mobile phase was 5 mM aqueous sulfuric acid at a flow rate of 0.55 mL min^{-1}. The HPLC column was operated at 60 °C. Since the products were not fully soluble in water, a water extraction step (proportion of 1 : 10 of ozonated lignin and water) was needed, and the aqueous phase was further analyzed. Calibration curves of the targeted acids were determined experimentally to provide an accurate quantification and were based on a minimum of 4 data points with excellent linear fitting (*i.e.* $R^2 > 0.99$).

Heteronuclear single quantum coherence (HSQC) NMR spectra were acquired on a Bruker NMR spectrometer (600 MHz) with the following parameters: 11 ppm sweep width in F2 (^{1}H), 220 ppm sweep width in F1 (^{13}C), 8 scans and a total

acquisition time of around 1 h. Sample preparation involved the dissolution of the sample in DMSO-d_6 (15 wt%). Spectra were processed and analyzed using MestReNova software, refer to the ESI† for integration details.

^{13}C-NMR spectra were acquired on a Bruker NMR spectrometer (600 MHz) using a 90° pulse and an inverse-gated decoupling sequence with relaxation delay of 5 seconds, sweep width of 220 ppm and 2048 scans, with a total acquisition time of 3.5 h and TMS as reference. Sample preparation involved the dissolution of the sample in DMSO-d_6 (15 wt%). Spectra were processed and analyzed using MestReNova software, refer to the ESI† for integration details.

Hydroxyl content analyses were performed using ^{31}P-NMR following a procedure described elsewhere,[7] using cyclohexanol as the internal standard and $CDCl_3$ as solvent. ^{31}P-NMR spectra were acquired on a Bruker NMR spectrometer (600 MHz) at 293 K using a standard 90° pulse, 256 scans and 5 s of relaxation delay. Spectra were processed and analyzed using MestReNova software, refer to the ESI† for integration details.

The water content was determined by Karl Fischer titration using a Metrohm 702 SM Titrino titration device. About 0.01 g of sample was injected in an isolated glass chamber containing Hydranal (Karl Fischer solvent, Riedel de Haen). The titrations were carried out using the Karl Fischer titrant Composit 5K (Riedel de Haen). All analyses were performed at least 3 times and the average value is reported.

Elemental analysis (C, H, N, S) was performed using a Euro-Vector EA3400 Series CHN–O analyzer with acetanilide as the reference. The oxygen content was determined by difference. All analyses were carried out at least in duplicate and the average value is reported.

Dynamic light scattering (DLS) measurements were performed using a Brookhaven Zeta-PALS analyzer equipped with a 35 mW red diode laser (nominal wavelength of 660 nm), reading at a measurement angle of 90°. The measurements were carried out on aqueous colloidal solutions (1 wt% of lignin concentration) at 25 °C. The mean effective diameter of each lignin sample (*i.e.* particle size) was obtained after 10 measurements assuming that the particles are spherically shaped.

Results and discussion

Characterization of the lignin feeds

Table 1 shows relevant properties of the four lignins used in the ozonation experiments, which were characterized in detail by GPC, NMR techniques, elemental analysis and DLS. These lignins can be separated in two subsets, *i.e.* a subset comprised of softwood derived G-based Kraft lignins (KL and ball-milled KL) and a subset comprised of mixed S/G-based organosolv lignins (Alcell and Fabiola). Apart from the differences in monomer unit composition, KL and ball-milled KL also present relatively higher contents of sulphur and nitrogen as well as

Table 1 Relevant properties of the technical lignins used in this study

Property	KL	Ball-milled KL	Alcell	Fabiola
M_w (g mol^{-1})	1212	1051	2017	1683
Elemental composition (wt%, dry basis)				
C	62.2	61.75	65.65	63.42
H	6.00	5.96	6.14	5.87
N	0.75	0.77	0.14	0.06
O	29.80	29.90	27.80	30.61
S	1.20	1.61	0.26	0.05
S/G/H ratio (%)[a]	0/97.5/2.5	0/97.7/2.3	67/31.7/1.3	68.9/30.5/0.5
$S_{condensed}$ units (%)[a]	—	—	16.9	13
β-O-4 linkages (%)[a]	10.6	9.9	13.8	19.5
β-5 linkages (%)[a]	2.2	1.9	3.5	3.8
β–β linkages (%)[a]	4.1	4.3	8.2	10.5
Aliphatic C–H (area%)[b]	13.1	11	17.1	3.9
Aliphatic C–O (area%)[b]	18.2	15.7	11.6	10.5
Aromatic-OCH_3 (area%)[b]	12.7	14.8	18.3	32
Aromatic C–H (area%)[b]	29.5	32.3	26.6	28.9
Aromatic C–C (area%)[b]	14.9	16	17.5	18.8
Aromatic C–O (area%)[b]	10.4	10.1	8.8	5.9
Carbonyl (area%)[b]	1.2	0	0	0
OH aliphatic (mmol g^{-1})[c]	2.53	2.44	1.66	2.53
OH C_5 substituted units (mmol g^{-1})[c]	0.30	0.81	0.73	1.04
OH S-units (mmol g^{-1})[c]	—	—	0.92	0.99
OH G-units (mmol g^{-1})[c]	0.58	0.60	0.45	0.43
OH phenolics (mmol g^{-1})[c]	0.17	0.09	0.10	0.02
OH acids (mmol g^{-1})[c]	0.03	—	0.02	—
Particle size (nm)[d]	1080	460	930	790

[a] As determined by HSQC NMR, refer to ESI for details. [b] As determined by ^{13}C-NMR, refer to ESI for details. [c] As determined by ^{31}P-NMR, refer to ESI for details. [d] Mean value as determined by DLS measurements.

a lower M_w. The first subset provides a comparison regarding the average particle size (*i.e.* 1080 nm *versus* 460 nm). Besides the slightly lower M_w of the ball-milled KL, no significant differences were observed between the properties of KL and ball-milled KL, showing that the conditions applied in the ball-milling step prevented major structural changes. Furthermore, the low β-O-4 content of KL likely did not allow for further lignin degradation, as specifically these linkages were shown to be prone to cleavage during ball-milling.[64,65]

The second subset compares two lignins which mainly have a different level of condensation. Accordingly, the Fabiola lignin used in this study is less condensed than the Alcell lignin due to the milder conditions applied in the organosolv process.[63] This is confirmed by its higher oxygen content, higher amount of C–O linkages (mainly β-O-4, in line with the higher amount of aliphatic OH provided by ^{31}P-NMR) and lower amount of $S_{condensed}$ units shown by HSQC NMR analysis. Furthermore, ^{13}C-NMR results shows significantly less aliphatic C–H motifs in the Fabiola lignin and relatively more methoxy groups attached to aromatic rings, also suggesting a structure that resembles more native lignin. In addition to that, the results from ^{31}P-NMR show a lower amount of phenolic OH groups (which are known to increase with lignin degradation[61,66,67]) in this lignin.

Product yields and macromolecular properties

To demonstrate the reactivity of ozone towards these technical lignins, each was exposed to ozone for different times (20 min to up to 60 or 120 min, Fig. 3). All experiments were performed under ambient conditions by bubbling ozone through a suspension of the lignin in ethanol. The experiment reacting KL with ozone for 20 min was performed in triplicate to investigate reproducibility and showed good results (standard deviation of 0.7% on the measured weight of the different product fractions). Clear visual changes were observed during the experiments, indicating promising reactivity at these mild, non-catalytic reaction conditions. For instance, all the lignins initially present low solubility in ethanol (varying between 4–33 wt%, see blank runs without ozone in Fig. 3) which increased dramatically upon ozone exposure, and the ozonated solutions turned orange-red. The lignin oils after ethanol removal show a clear difference from the starting dark brown solid lignins, being a low viscosity oil with an orange-red color (see Fig. S2† for an example). Accordingly, the lighter color is related to the decrease of conjugated aromatic structures and thus indicates reactivity at unsaturations.[68]

Fig. 3 also shows that the lignin oil yields significantly surpass the amount of dissolved lignin after ozonation. Such mass increase is a direct result of oxygen incorporation into the structure and also suggests that the solvent participates in some reaction pathways. For instance, solvent incorporation was previously observed when using methanol as the solvent.[59] In a similar fashion, ethanol may be incorporated *via* ester and acetal formation reactions of the acids and aldehydes/ketones respectively, which are all formed during ozonation (*vide infra*). Furthermore, ethanol might also serve as a capping agent that stabilizes highly reactive (oxidized) phenolic intermediates by O-alkylation of hydroxyl groups.[69,70] Average incorporation ratios of 2.0, 1.9, 1.8 and 2.1 were observed for KL, ball milled KL, Alcell and Fabiola lignin, respectively. This indicates that for a determined amount of lignin solubilized during ozonation, the amount of lignin oil after ethanol removal will be approximately doubled.

Since significant mass incorporation occurs, precise mass balances are obscured and both the yields of lignin oil and insoluble lignin have to be evaluated. For instance, the yields of lignin oil showed an overall increase with longer ozonation times, and results varied distinctly among the lignins (Fig. 3, O3 entries). For the KL, ball-milled KL and Alcell lignins, the high yields of lignin oil were accompanied by desirable low amounts of insoluble lignin after ozonation. Alcell lignin showed the

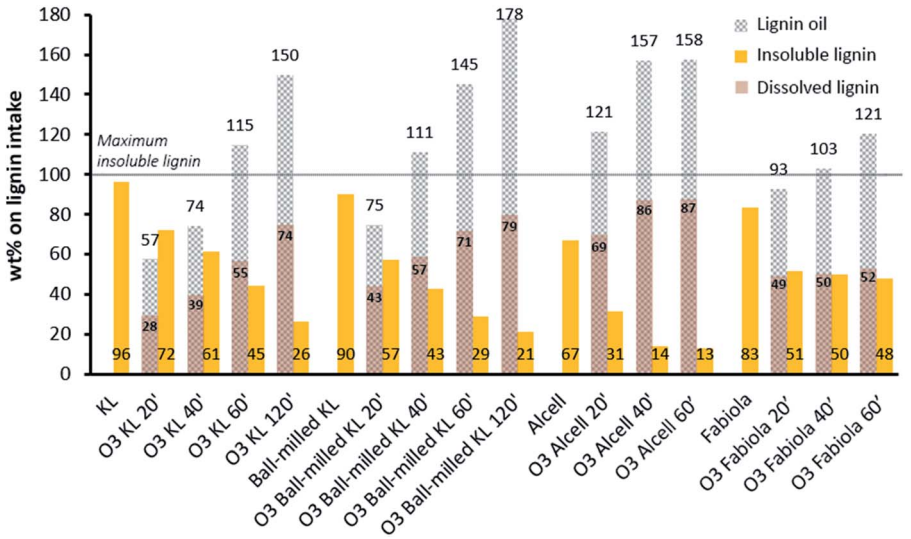

Fig. 3 Yields of lignin oil, insoluble lignin and dissolved lignin for the lignin feed blank runs and different reaction times (minutes) with ozone (O3 entries).

least solid residue (13 wt%) and thus highest dissolved lignin which might relate to its relatively higher initial solubility in ethanol, being itself an ethanol/water extracted lignin.

As the lignins are nearly insoluble in ethanol, mass transfer limitations of ozone from the gas to the liquid phase and subsequent transfer to the solid lignin particles play an important role in this system and may determine the overall rate of the reactions. The use of ball-milled KL with a significantly smaller particle size led to a slightly higher initial lignin solubility and indeed an overall increased solvation and less insoluble residual lignin compared to KL. This is likely due to better dispersion and a higher surface area, facilitating reactions to take place. It is expected that optimized set-ups with proper attention to mass transfer issues (*e.g.* intense mechanical stirring using overhead, self-inducing expellers) may lead to higher lignin oil yields at shorter reaction times.

For the Fabiola lignin, a plateau for the amounts of dissolved lignin was observed from 20 to 60 minutes of reaction time, in which relatively low yields of lignin oil and high amounts of insoluble lignin (*i.e.* around 50 wt%) were observed. This surprising result is likely related to the structural features of this lignin. For instance, the milder organosolv extraction procedure used for this lignin (compared to the Alcell process) results in a structure more similar to native lignin,[71,72] *i.e.* less condensed and with a higher amount of C–O bonds and methoxy groups (*vide supra*, Table 1). Literature shows that C–O linked lignins are usually easier to depolymerize, as C–O bonds are more labile when compared to C–C bonds.[73–75] Nonetheless, the apparently contradictory results here observed can be explained by specific reactivity trends of ozone. A recent publication from our group showed that the β-O-4 linking motifs are relatively resistant to ozone attack, and that the major influence for lignin disruption during ozonation particularly comes from available phenolic hydroxy groups.[59] Such phenolic groups are mostly the results of structural modifications of native lignin during processing.[61,66,67,76] Furthermore, the presence of C–C double bonds (*i.e.* stilbene linkages) as reported in Kraft lignin[61,77,78] increases its reactivity towards ozone due to the high electronic density of such moieties.[79,80] Hence, in the case of an ozone treatment, condensed structures as in technical lignins (*i.e.* Kraft and Alcell lignins) are beneficial for their reactivity and subsequent dissolution in ethanol, leading to the higher lignin oil yields observed.

GPC analyses were performed to compare the molecular weight distribution of the lignin feeds and their ozonated lignin oils (Fig. 4). The results clearly show that the lignin fragments being solubilized during ozonation are substantially lower in molecular weight compared to the initial lignin feed, indicating that ozone simultaneously breaks down the structure and increases its solubility in ethanol. Furthermore, repolymerization pathways usually observed in oxidative processes due to the formation of radicals[30,81] seem to be suppressed as no molecular weight increase was observed at elongated reaction times. This positive observation is likely a result of the acidic reaction medium and solvent system used, as ethanol is reportedly an efficient radical scavenger able to quench reactive lignin fragments[70,82,83] under such conditions. Accordingly, while the mixture of ethanol and KL before reaction was slightly acidic (average pH of 6, standard error of 0.1), the lignin oil solution after ozonation for 20 minutes had a substantially higher acidity (average pH of 2.3, standard error of 0.1). Lignin-solvent reactions may also play a role on inhibiting competitive repolymerization pathways.[48] For most cases, increasing the reaction time from 20 to 60 minutes led to an increase of the lower M_w fractions due to the subsequent oxidation of the lignin fragments solubilized in ethanol, which is known to happen at

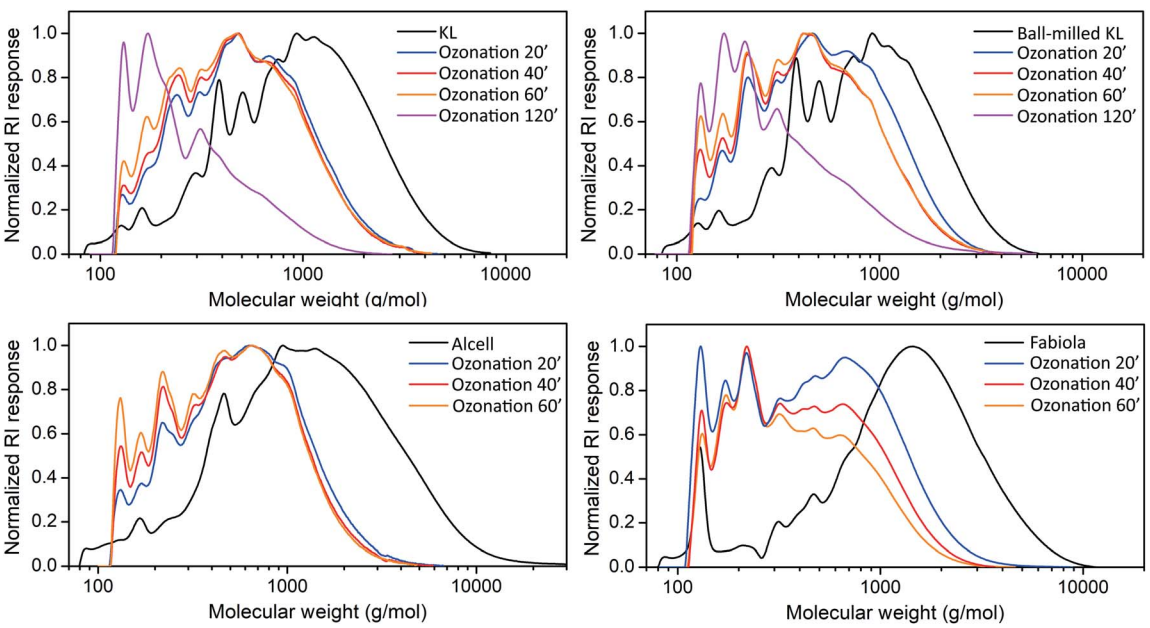

Fig. 4 GPC (THF) results for the lignin feeds and their corresponding lignin oils after different ozonation times (minutes).

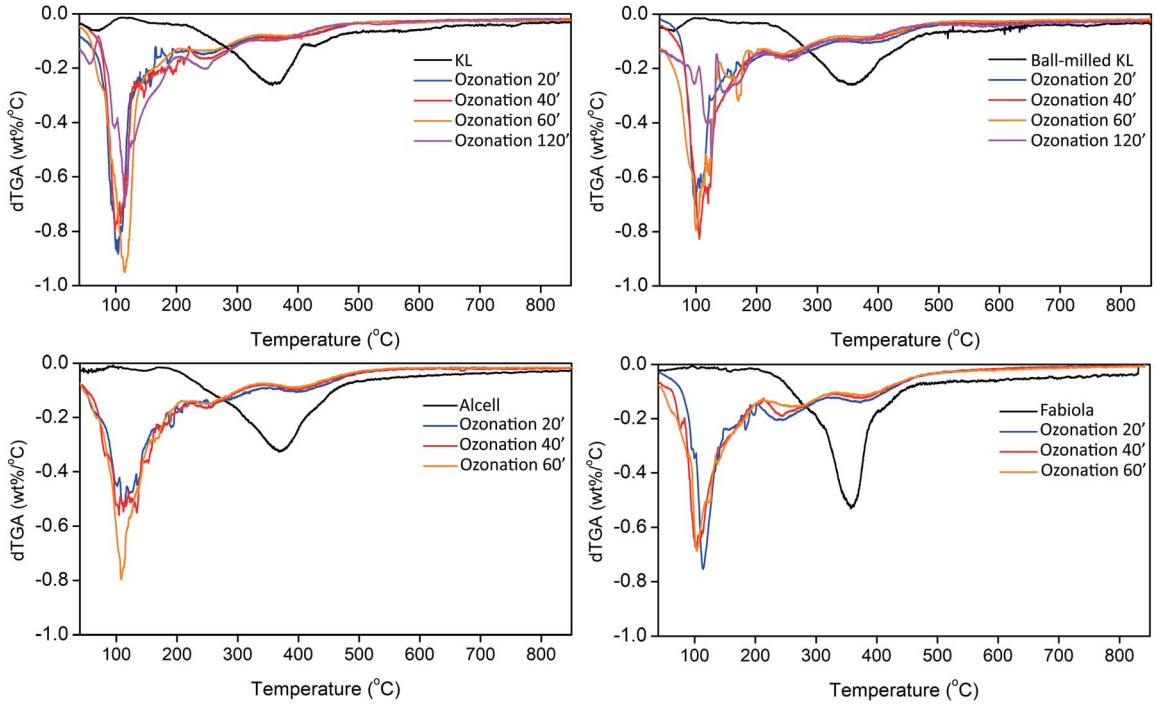

Fig. 5 dTGA results for the lignin feeds and their corresponding lignin oils after different ozonation times (minutes).

extended ozonation times.[54,55,59] The amounts of these fractions were greatly increased at the longer reaction times of 120 minutes (KL and ball-milled KL), likely accompanied by carbon loss due to CO_2 formation from over-oxidation.[84] As set-up limitations hindered an accurate analyses of the gaseous products, full mass and carbon balances could not be determined. An overall decrease of 40–75% in the M_w (based on the initial M_w of each lignin) ratify the high activity of ozone towards lignin structures and that no substantial repolymerization of the solubilized ozonated fragments occurs.

TGA results are in line with GPC, showing a substantial increase in volatility due to depolymerization (Fig. 5 and S3†). Accordingly, the amounts of non-volatiles decreased by 60–80% (based on the initial TGA non-volatile residue of each lignin) with the ozone treatment, being of around 10 wt% after ozonation. No substantial variation on the TGA residue was observed under the different reaction times applied. Furthermore, the temperature of maximum mass loss shifted from around 350–400 °C to values lower than 250 °C. These results ratify the extensive depolymerization of lignin and show that the smaller fragments produced are also more volatile and thermally stable, since no substantial repolymerization was observed under the high temperatures applied during TGA. Such lowered charring tendency is of great interest for fuel and fuel additives applications.[55,85]

Elemental analyses showed large differences in the composition of the lignin oils when compared to their former lignins. Results are displayed in a Van Krevelen plot, see Fig. 6. For instance, the O/C ratio increase is expected as more oxygen is incorporated into the lignin structure, and the H/C ratio increase is likely a result of ethanol incorporation *via* esterification reactions (which are accompanied by water formation). Despite possible water losses during ethanol removal, positive correlations could be observed when plotting the H/C molar ratios *versus* the water contents determined for the lignin oils (Fig. S4†). Having the Alcell data as reference, an estimated value of 36 wt% of the total mass incorporation after ozonation for 60 minutes could be attributed to the incorporation of ethanol *via* esters and acetals.

Lignin oil composition and structural transformations

Chromatographic analyses were performed on the lignin oils to identify and quantify low molecular weight products. GC-MS qualitative analyses show an extensive formation of (di)ethyl

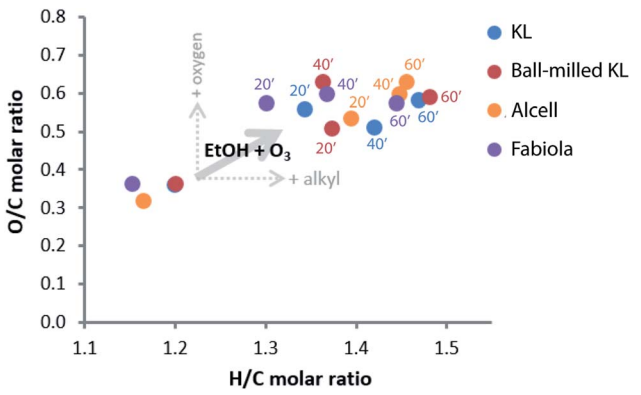

Fig. 6 Van Krevelen plot of the lignin feeds and lignin oils after ozonation.

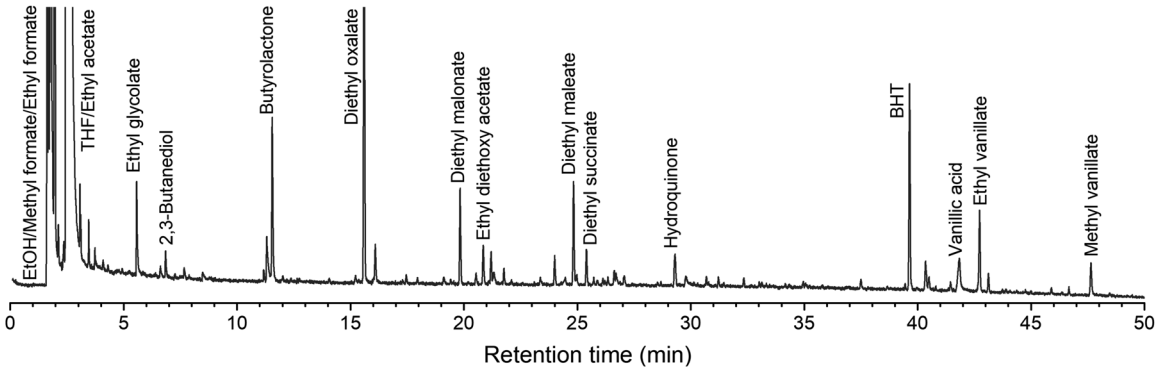

Fig. 7 Representative GC-MS chromatogram of a lignin oil (ball-milled KL ozonated for 60 minutes). Butylated hydroxytoluene (BHT) is the stabilizer present in the THF (solvent).

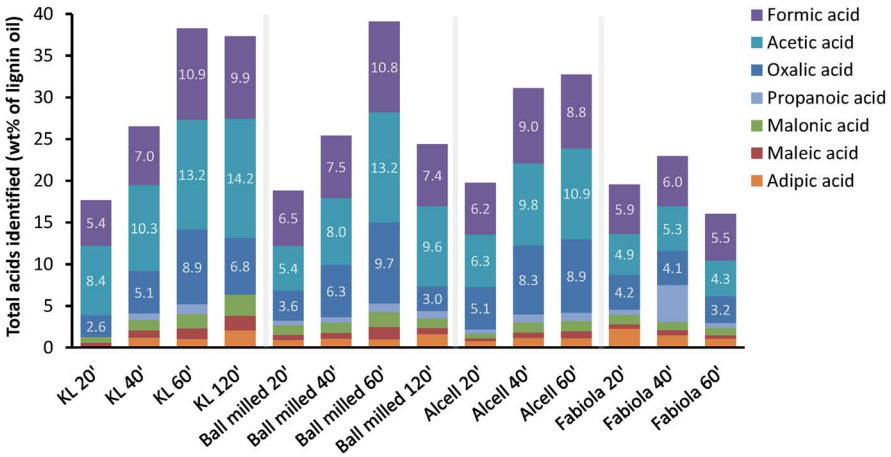

Fig. 8 Main (di)carboxylic acids identified by HPLC analysis of the obtained product oils under hydrolysis conditions.

esters in the volatile and thermally stable fraction (Fig. 7). This confirms that ethanol is incorporated in the products mainly through esterification reactions of the (di)carboxylic acids produced, being these a result of ring-opening reactions largely favored by ozone.[54,55] Such observations are in line with elemental analyses results (*vide supra*) and with a previous study from our group, in which (di)methyl esters were identified after

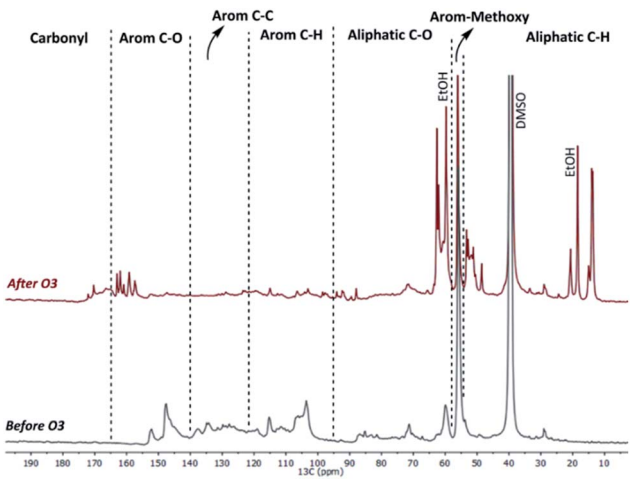

Fig. 9 Representative ^{13}C-NMR spectra (DMSO-d_6) of the Fabiola lignin and its lignin oil (1 h ozonation time).

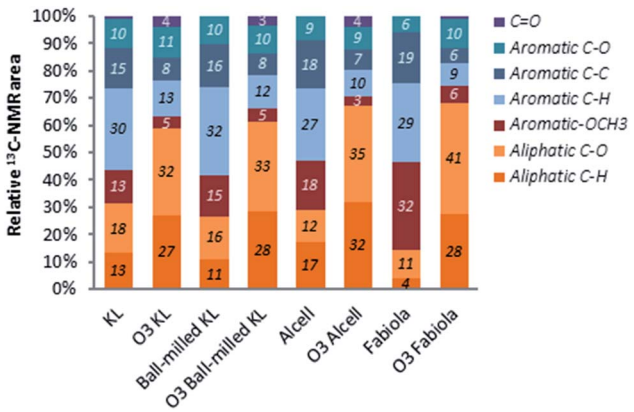

Fig. 10 ^{13}C-NMR integration results for the lignin feeds and lignin oils (1 h ozonation time).

exposing a solution of pyrolytic lignin and methanol to ozone.[59] Acetals and aromatic oxidation products were also identified, *e.g.* vanillic acid, ethyl vanillate and hydroquinone.

Through an extraction of the product oil with water and subsequent HPLC analyses of the obtained aqueous phase, a range of (di)carboxylic acids could be identified and

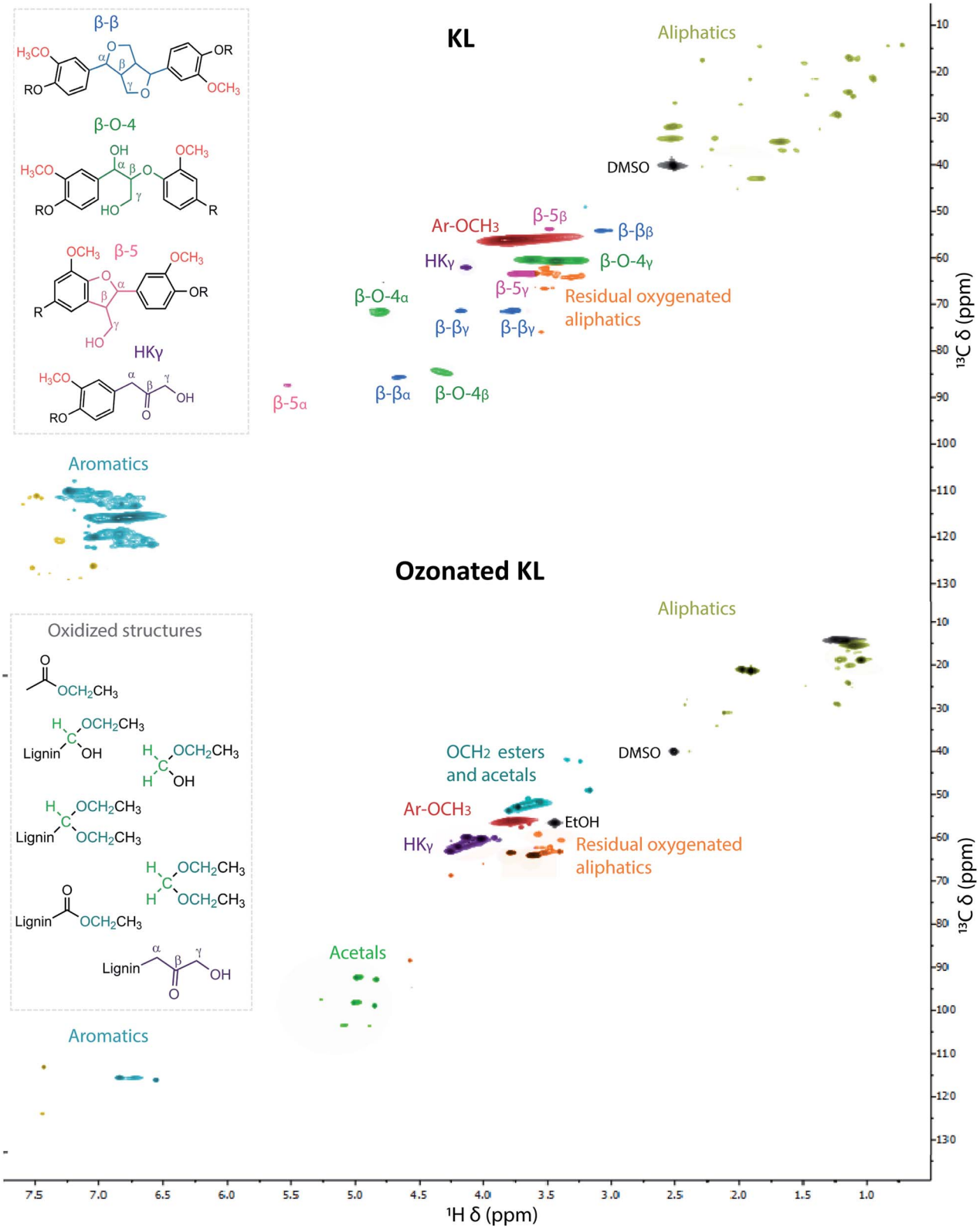

Fig. 11 HSQC NMR spectra (DMSO-d_6) for KL and its lignin oil (1 h ozonation time).

quantified (Fig. 8 and Table S3†). Importantly, as the HPLC analyses were performed under hydrolysis conditions, it was not possible to quantify acids and esters separately. Overall, the yields of these organic acids increased with ozonation time and reached up to 40 wt% of the lignin oil. Minor amounts of formic and acetic acid arise from the oxidation of ethanol. This was proven by blank ozonation experiments with ethanol (reaction times of 20/40/60 minutes) that yielded 0.9/1.2/1.4 wt% and 1.6/2.2/2.8 wt% of formic and acetic acid, respectively. The decrease in detected acids at longer reaction times (*i.e.* 120 minutes for the ball-milled KL and 60 minutes for the Fabiola lignin) might be related to the over-oxidation of small (di)carboxylic acids to CO_2. [84] In general, the chromatographic analyses show that the low molecular weight products produced during ozonation are largely a result of lignin conversion into (di)carboxylic acids, which are esterified to their respective (di)ethyl esters due to the presence of ethanol in an acidic environment. In order to determine the chemical composition of the whole lignin oil rather than solely the lower molecular weight fraction, NMR analysis was used to further elucidate global structural transformations during ozonation. Representative ^{13}C-NMR spectra and the integration results of the lignin feeds and their lignin oils after 60 minutes of ozonation show substantial structural differences (Fig. 9 and 10).

Regardless of the lignin used, products were richer in aliphatic bonds after ozonation. While aliphatic C–O bonded carbons are a direct result of oxidation and ring opening reactions, the increase in C–H bonded carbons is related to the incorporation of ethanol within the structure. Aromatic carbons showed an overall decrease that varied between 40–55% depending on the lignin, and new carbon signals for carbonyl groups could be observed, being expected due to the formation of (di)carboxylic acids and esters. The substantial decrease in methoxy groups attached to aromatics is also an indication of ring-opening reactions. Importantly, while the distribution of bonds in the lignin oils is similar in all cases, variations in the yields depending on the lignin substrate used must be recalled in order to select an adequate feed for ozonation. When considering such aspects, the ball-milled Kraft and Alcell lignins are the most promising options, as a large fraction of them (*i.e.* 71–87 wt%) was solubilized by the ozone mediated depolymerization under the applied conditions (*vide supra*).

Qualitative results provided by HSQC NMR ratify the aromatic disruption, as well the disappearance of well-defined linkages typically found in lignin (*i.e.* β–β, β-5, β-O-4),[71] see Fig. 11 for a representative spectra of KL and its lignin oil (1 h ozonation) and Fig. S5–S7† for the spectra of the lignin oils obtained from the other feeds. Overall, similar trends were observed that relate to the formation of ethyl esters, acetals and aliphatic chains containing carbonyl and hydroxyl groups. In addition, the aliphatic C–H region is less heterogeneous (as C–O linkages were formed) and contained just a few signals, which are mostly derived from ethanol incorporation. NMR and GC-MS analyses of a blank ozonation experiment with ethanol indicated the formation of some acids, esters and acetals (Fig. S8–S10†) which can contribute to the observed signals and are in line with the results previously observed using methanol.[59]

Fig. 12 illustrates the findings of this work in a scheme. Overall, it was shown that technical lignins could be converted in high yields into ethanol-soluble fragments by an ozone mediated depolymerization operated under room conditions. The obtained lignin oils have significant lower M_w and a less aromatic character due to ring-opening reactions. A range of low molecular weight compounds was identified, particularly DCAs and their derived (di)ethyl esters. Both ethanol and ozone are incorporated to give esters and acetals as main functional groups in the product mixture. Various applications in the food and pharma industries are envisioned for the DCAs,[33] while esters can be used as high value fuels and additives.[55] Furthermore, there is great potential for obtaining lignin-based materials from ozonated fragments[58] and oxygenated aromatics.[86]

Conclusions

The results presented here clearly show the potential of ozonation for breaking down recalcitrant technical lignins and promoting their solvation in ethanol, which is a recyclable and biobased solvent option with low toxicity. Accordingly, the Kraft and organosolv lignins evaluated were converted under ambient conditions and without the need of catalysts. Lower particle sizes favored higher yields due to the increased contact areas and better dispersion of the lignin particles in the liquid medium. Furthermore, increased structural degradation of the native lignin structure prior to ozonation was shown to be beneficial for the effective conversion of the lignin feed. This is likely due to the increased amounts of reactive phenolic motifs and C–C double bonds in comparison with native lignin. Both Kraft and Alcell lignins were shown to be suitable feeds for the process, leading to high lignin

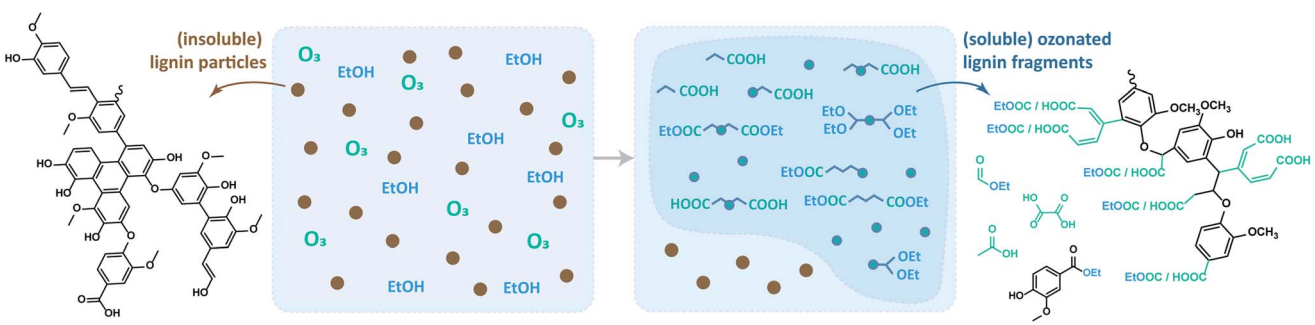

Fig. 12 Scheme of the ozone mediated depolymerization of lignin.

oil yields containing up to 40 wt% of low molecular weight compounds. The depolymerized lignin fragments have a substantially lower M_w (*i.e.* 40–75%) and much higher volatility compared with their former lignins. While ozonation favored phenol ring-opening pathways that produce (di)carboxylic acids, ethanol was shown to suppress repolymerization pathways and incorporate within the lignin structure mostly as ethoxy groups in esters and acetals. Longer reaction times led to higher yields of small (di) carboxylic acids/esters, and likely the over-oxidation of some molecules to CO_2. These results clearly show that ozonation is effective in converting recalcitrant technical lignins into ethanol-soluble fragments containing valuable monomers and oligomers with a more aliphatic character. Further in-depth studies of crucial process parameters (*i.e.* ozone input, residence time, stirring speed) may tune the product distribution towards the desired applications. Accordingly, the use of optimized set-ups can minimize mass transfer limitations, suppressing undesired secondary reactions in the liquid phase and providing a more efficient use of ozone. Within the biorefinery concept, which aims to synergistically valorize all biomass fractions, lignin ozonation can serve both as a way to produce valuable oxygenated products (*e.g.* DCAs) and as a straightforward pretreatment to depolymerize, solubilize and make the lignin structure more accessible for further processing by strategies typically hampered by its recalcitrance (*e.g.* hydrotreatment). Due to the high ester content, H/C ratio and volatility, ozonation can be a starting point for converting technical lignins into oils suitable for applications as fuels and fuel additives.

Conflicts of interest

There are no conflicts to declare.

Acknowledgements

Financial support from the Science without Borders program (CNPq, Brazil) for the PhD project of M.B.F. is gratefully acknowledged. We also thank Erwin Wilbers, Marcel de Vries, Léon Rohrbach and Jan Henk Marsman for the technical support. Hans van der Velde is gratefully acknowledged for performing the elemental analyses. We thank Arjan Smit (ECN, TNO) for providing the Fabiola lignin used in this study and Shilpa Agarwal for providing the ball-milled KL used in this study for which she acknowledges the use of equipment owned by University of Twente.

References

1 A. J. Ragauskas, G. T. Beckham, M. J. Biddy, R. Chandra, F. Chen, M. F. Davis, B. H. Davison, R. A. Dixon, P. Gilna, M. Keller, P. Langan, A. K. Naskar, J. N. Saddler, T. J. Tschaplinski, G. A. Tuskan and C. E. Wyman, *Science*, 2014, **344**, 1246843.
2 R. J. A. Gosselink, E. de Jong, B. Guran and A. Abächerli, *Ind. Crops Prod.*, 2004, **20**, 121–129.
3 H. Wang, Y. Pu, A. Ragauskas and B. Yang, *Bioresour. Technol.*, 2019, **271**, 449–461.
4 F. S. Chakar and A. J. Ragauskas, *Ind. Crops Prod.*, 2004, **20**, 131–141.
5 P. C. A. Bruijnincx, R. Rinaldi and B. M. Weckhuysen, *Green Chem.*, 2015, **17**, 4860–4861.
6 R. Rinaldi, R. Jastrzebski, M. T. Clough, J. Ralph, M. Kennema, P. C. A. Bruijnincx and B. M. Weckhuysen, *Angew. Chem., Int. Ed.*, 2016, **55**, 8164–8215.
7 S. Constant, H. L. J. Wienk, A. E. Frissen, P. de Peinder, R. Boelens, D. S. van Es, R. J. H. Grisel, B. M. Weckhuysen, W. J. J. Huijgen, R. J. A. Gosselink and P. C. A. Bruijnincx, *Green Chem.*, 2016, **18**, 2651–2665.
8 M. V. Galkin and J. S. M. Samec, *ChemSusChem*, 2016, **9**, 1544–1558.
9 J. Zakzeski, P. C. Bruijnincx, A. L. Jongerius and B. M. Weckhuysen, *Chem. Rev.*, 2010, **110**, 3552–3599.
10 C. R. Kumar, N. Anand, A. Kloekhorst, C. Cannilla, G. Bonura, F. Frusteri, K. Barta and H. J. Heeres, *Green Chem.*, 2015, **17**, 4921–4930.
11 A. Narani, R. Kumar Chowdari, C. Cannilla, G. Bonura, F. Frusteri, H. Jan Heeres and K. Barta, *Green Chem.*, 2015, **17**, 5046–5057.
12 A. Oasmaa, R. Alén and D. Meier, *Bioresour. Technol.*, 1993, **45**, 189–194.
13 I. Hita, P. J. Deuss, G. Bonura, F. Frusteri and H. J. Heeres, *Fuel Process. Technol.*, 2018, **179**, 143–153.
14 J. Yang, L. Zhao, S. Liu, Y. Wang and L. Dai, *Bioresour. Technol.*, 2016, **212**, 302–310.
15 L. Jin, W. Li, Q. Liu, J. Wang, Y. Zhu, Z. Xu, X. Wei and Q. Zhang, *Fuel Process. Technol.*, 2018, **178**, 62–70.
16 J. Yang, L. Zhao, C. Liu, Y. Wang and L. Dai, *Bioresour. Technol.*, 2016, **218**, 926–933.
17 A. Kloekhorst and H. J. Heeres, *ACS Sustainable Chem. Eng.*, 2015, **3**, 1905–1914.
18 A. Kloekhorst, Y. Shen, Y. Yie, M. Fang and H. J. Heeres, *Biomass Bioenergy*, 2015, **80**, 147–161.
19 S. Agarwal, R. K. Chowdari, I. Hita and H. J. Heeres, *ACS Sustainable Chem. Eng.*, 2017, **5**, 2668–2678.
20 I. Hita, H. J. Heeres and P. J. Deuss, *Bioresour. Technol.*, 2018, **267**, 93–101.
21 S. Qiu, M. Li, Y. Huang and Y. Fang, *Ind. Eng. Chem. Res.*, 2018, **57**, 2023–2030.
22 T. I. Korányi and E. J. M. Hensen, *Catal. Lett.*, 2017, **147**, 1722–1731.
23 R. Ma, W. Hao, X. Ma, Y. Tian and Y. Li, *Angew. Chem., Int. Ed.*, 2014, **53**, 7310–7315.
24 R. K. Chowdari, S. Agarwal and H. J. Heeres, *ACS Sustainable Chem. Eng.*, 2019, **7**, 2044–2055.
25 J. Löfstedt, C. Dahlstrand, A. Orebom, G. Meuzelaar, S. Sawadjoon, M. V. Galkin, P. Agback, M. Wimby, E. Corresa, Y. Mathieu, L. Sauvanaud, S. Eriksson, A. Corma and J. S. M. Samec, *ChemSusChem*, 2016, **9**, 1392–1396.
26 C. Zhu, X. Dou, W. Li, X. Liu, Q. Li, J. Ma, Q. Liu and L. Ma, *Bioresour. Technol.*, 2019, **284**, 293–301.
27 W. Li, X. Dou, C. Zhu, J. Wang, H. Chang, H. Jameel and X. Li, *Bioresour. Technol.*, 2018, **269**, 346–354.
28 S. Gharehkhani, Y. Zhang and P. Fatehi, *Prog. Energy Combust. Sci.*, 2019, **72**, 59–89.
29 A. Rahimi, A. Azarpira, H. Kim, J. Ralph and S. S. Stahl, *J. Am. Chem. Soc.*, 2013, **135**, 6415–6418.

30 T. Voitl and P. RudolfvonRohr, *ChemSusChem*, 2008, **1**, 763–769.
31 Y. Zhao, Q. Xu, T. Pan, Y. Zuo, Y. Fu and Q.-X. Guo, *Appl. Catal., A*, 2013, **467**, 504–508.
32 T. Voitl and P. R. von Rohr, *Ind. Eng. Chem. Res.*, 2010, **49**, 520–525.
33 R. Ma, M. Guo and X. Zhang, *ChemSusChem*, 2014, **7**, 412–415.
34 W. Deng, H. Zhang, X. Wu, R. Li, Q. Zhang and Y. Wang, *Green Chem.*, 2015, **17**, 5009–5018.
35 H. Deng, L. Lin, Y. Sun, C. Pang, J. Zhuang, P. Ouyang, J. Li and S. Liu, *Energy Fuels*, 2009, **23**, 19–24.
36 Z. Bi, Z. Li and L. Yan, *Green Process. Synth.*, 2018, **7**, 306–315.
37 J. Mottweiler, M. Puche, C. Räuber, T. Schmidt, P. Concepción, A. Corma and C. Bolm, *ChemSusChem*, 2015, **8**, 2106–2113.
38 C. Zhu, W. Ding, T. Shen, C. Tang, C. Sun, S. Xu, Y. Chen, J. Wu and H. Ying, *ChemSusChem*, 2015, **8**, 1768–1778.
39 C. Crestini, R. Saladino, P. Tagliatesta and T. Boschi, *Bioorg. Med. Chem.*, 1999, **7**, 1897–1905.
40 S. C. Patankar, L.-Y. Liu, L. Ji, S. Ayakar, V. Yadav and S. Renneckar, *Green Chem.*, 2019, **21**, 785–791.
41 R. Prado, A. Brandt, X. Erdocia, J. Hallet, T. Welton and J. Labidi, *Green Chem.*, 2016, **18**, 834–841.
42 G. Chatel and R. D. Rogers, *ACS Sustainable Chem. Eng.*, 2014, **2**, 322–339.
43 J. Zakzeski, A. L. Jongerius and B. M. Weckhuysen, *Green Chem.*, 2010, **12**, 1225–1236.
44 T. Vangeel, W. Schutyser, T. Renders and B. F. Sels, *Top. Curr. Chem.*, 2018, **376**, 30.
45 M. Zhang, F. L. P. Resende, A. Moutsoglou and D. E. Raynie, *J. Anal. Appl. Pyrolysis*, 2012, **98**, 65–71.
46 A. Tumbalam Gooty, D. Li, F. Berruti and C. Briens, *J. Anal. Appl. Pyrolysis*, 2014, **106**, 33–40.
47 J. A. Caballero, R. Font and A. Marcilla, *J. Anal. Appl. Pyrolysis*, 1997, **39**, 161–183.
48 J. B. Nielsen, A. Jensen, C. B. Schandel, C. Felby and A. D. Jensen, *Sustainable Energy Fuels*, 2017, **1**, 2006–2015.
49 C. Løhre, G.-A. A. Laugerud, W. J. J. Huijgen and T. Barth, *ACS Sustainable Chem. Eng.*, 2018, **6**, 3102–3112.
50 C. Løhre, T. Barth and M. Kleinert, *J. Anal. Appl. Pyrolysis*, 2016, **119**, 208–216.
51 B. Holmelid, T. Barth, R. Brusletto and M. Kleinert, *Biomass Bioenergy*, 2017, **105**, 298–309.
52 W. M. Goldmann, J. M. Anthonykutty, J. Ahola, S. Komulainen, S. Hiltunen, A. M. Kantola, V.-V. Telkki and J. Tanskanen, *Waste Biomass Valorization*, 2019, 1–12.
53 R. Ma, Y. Xu and X. Zhang, *ChemSusChem*, 2015, **8**, 24–51.
54 M. Ragnar, T. Eriksson, T. Reitberger and P. Brandt, *Holzforschung*, 1999, **53**, 423–428.
55 C. J. Chuck, H. J. Parker, R. W. Jenkins and J. Donnelly, *Bioresour. Technol.*, 2013, **143**, 549–554.
56 J. Quesada, M. Rubio and D. Góamez, *J. High Resolut. Chromatogr.*, 1997, **20**, 565–568.
57 M. V. Bule, A. H. Gao, B. Hiscox and S. Chen, *J. Agric. Food Chem.*, 2013, **61**, 3916–3925.
58 S. Zhang, T. Liu, C. Hao, L. Wang, J. Han, H. Liu and J. Zhang, *Green Chem.*, 2018, **20**, 2995–3000.
59 M. B. Figueirêdo, P. J. Deuss, R. H. Venderbosch and H. J. Heeres, *ACS Sustainable Chem. Eng.*, 2019, **7**, 4755–4765.
60 M. B. Figueiredo, F. Keij, A. Hommes, P. J. Deuss, R. H. Venderbosch, J. Yue and H. J. Heeres, *ACS Sustainable Chem. Eng.*, DOI: 10.1021/acssuschemeng.9b04020.
61 C. S. Lancefield, H. L. J. Wienk, R. Boelens, B. M. Weckhuysen and P. C. A. Bruijnincx, *Chem. Sci.*, 2018, **9**, 6348–6360.
62 P. de Wild, R. V. der Laan, A. Kloekhorst and E. Heeres, *Environ. Prog. Sustainable Energy*, 2009, **28**, 461–469.
63 A. Smit and W. Huijgen, *Green Chem.*, 2017, **19**, 5505–5514.
64 A. Tolbert, H. Akinosho, R. Khunsupat, A. K. Naskar and A. J. Ragauskas, *Biofuels, Bioprod. Biorefin.*, 2014, **8**, 836–856.
65 H. Chang, E. B. Cowling and W. Brown, *Holzforschung*, 2009, **29**, 153–159.
66 S. Sun, Y. Huang, R. Sun and M. Tu, *Green Chem.*, 2016, **18**, 4276–4286.
67 R. El Hage, N. Brosse, L. Chrusciel, C. Sanchez, P. Sannigrahi and A. Ragauskas, *Polym. Degrad. Stab.*, 2009, **94**, 1632–1638.
68 J. Gierer, *Wood Sci. Technol.*, 1986, **20**, 1–33.
69 X. Huang, T. I. Korányi, M. D. Boot and E. J. M. Hensen, *ChemSusChem*, 2014, **7**, 2276–2288.
70 X. Huang, T. I. Korányi, M. D. Boot and E. J. M. Hensen, *Green Chem.*, 2015, **17**, 4941–4950.
71 D. S. Zijlstra, A. de Santi, B. Oldenburger, J. de Vries, K. Barta and P. J. Deuss, *J. Visualized Exp.*, 2019, e58575.
72 C. S. Lancefield, I. Panovic, P. J. Deuss, K. Barta and N. J. Westwood, *Green Chem.*, 2017, **19**, 202–214.
73 P. J. Deuss, M. Scott, F. Tran, N. J. Westwood, J. G. de Vries and K. Barta, *J. Am. Chem. Soc.*, 2015, **137**, 7456–7467.
74 C. S. Lancefield, O. S. Ojo, F. Tran and N. J. Westwood, *Angew. Chem., Int. Ed.*, 2015, **54**, 258–262.
75 C. S. Lancefield, G. M. M. Rashid, F. Bouxin, A. Wasak, W.-C. Tu, J. Hallett, S. Zein, J. Rodríguez, S. D. Jackson, N. J. Westwood and T. D. H. Bugg, *ACS Sustainable Chem. Eng.*, 2016, **4**, 6921–6930.
76 H. Kawamoto, *J. Wood Sci.*, 2017, **63**, 117.
77 D. J. Yelle and J. Ralph, *Int. J. Adhes. Adhes.*, 2016, **70**, 26–36.
78 J. C. del Río, J. Rencoret, A. Gutiérrez, H. Kim and J. Ralph, *Plant Physiol.*, 2017, **174**, 2072–2082.
79 W. Sun, X. Gao, B. Wu and T. Ombrello, *Prog. Energy Combust. Sci.*, 2019, **73**, 1–25.
80 J. Drugman, *J. Chem. Soc.*, 1906, **89**, 939–945.
81 D. H. Kim, Y. Pu, R. P. Chandra, T. J. Dyer, A. J. Ragauskas and P. M. Singh, *J. Wood Chem. Technol.*, 2007, **27**, 219–224.
82 C. Cheng, J. Wang, D. Shen, J. Xue, S. Guan, S. Gu and K. H. Luo, *Polymers*, 2017, **9**, 240.
83 X. Ouyang, T. Ruan and X. Qiu, *Fuel Process. Technol.*, 2016, **144**, 181–185.
84 S. Kuitunen, A. Kalliola, V. Tarvo, T. Tamminen, S. Rovio, T. Liitiä, T. Ohra-aho, T. Lehtimaa, T. Vuorinen and V. Alopaeus, *Holzforschung*, 2011, **65**, 587–599.
85 A. Skreiberg, Ø. Skreiberg, J. Sandquist and L. Sørum, *Fuel*, 2011, **90**, 2182–2197.
86 A. M. Danby, M. D. Lundin and B. Subramaniam, *ACS Sustainable Chem. Eng.*, 2018, **6**, 71–76.

